Investigation of optical turbulence in the atmospheric surface layer using scintillometer measurements along a slant path and comparison to ultrasonic anemometer measurements

D. Sprung[1], E. Sucher[1], A. Ramkilowan[2],and D.J. Griffith[2]

[1]Fraunhofer IOSB (Institute of Optronics, System Technologies, and Image Exploitation), Gutleuthaustr. 1, 76275 Ettlingen, Germany, detlev.sprung@iosb.fraunhofer.de

[2]Optronic Sensor Systems (OSS), Defence, Peace Safety and Security (DPSS), Council for Scientific and Industrial Research (CSIR) P O Box 395, Pretoria 0001, South Africa dgriffith@csir.co.za

ABSTRACT

Optical turbulence represented by the structure function parameter of the refractive index C_n^2 is a relevant parameter for the performance of electro-optical systems and characterization of the atmospheric influence on imaging. It was investigated during a field trial above an Highveld grassland in the atmospheric surface layer at the Rietvlei Nature Reserve close to Pretoria in South Africa from 18th June to 30th June 2013. This campaign was performed to compare different measurement techniques analyzing the diurnal formation of the vertical distribution of optical turbulence up to a height of 16 m above ground. The chosen time period was characterized by a pronounced diurnal cycle of the meteorological conditions, i.e. low variations from day to day. Ultra sonic anemometers were used to measure high frequency time series (50 Hz) of temperature at single points. From the statistical analysis of these time series C_n^2 was derived. Three instruments were mounted at a portable mast in the center of slant path measurements over a horizontal distance of 1000 m using large aperture scintillometers (Boundary layer scintillometer BLS 900). Averaging over a time period of 5 minutes, the results of both methods are compared. The agreement in the results of optical turbulence is quite good. Discrepancies and agreement are analyzed with respect to the atmospheric stability and other meteorological parameters. Lowest values of C_n^2 at 4.6 m above ground amount to about $8*10^{-17}$ $m^{-2/3}$, daily maxima to $6*10^{-13}$ $m^{-2/3}$. Additional to the nearly constant meteorological conditions in the diurnal cycle, the uniformity of the terrain let the results of this measurement campaign an ideal data set for investigating methodological questions regarding a comparison of single point measurements with integrated measurements over a horizontal distance. Four stability regimes were identified in the diurnal cycle and investigated. These are convective conditions during the day, neutral conditions about sunrise and sunset, and two different stable regimes at night.

Keywords: optical turbulence, height dependence, boundary layer scintillometer, ultra sonic anemometer, comparison of measurement techniques, deep turbulence

Remote Sensing of Clouds and the Atmosphere XIX; and Optics in Atmospheric Propagation and Adaptive Systems XVII, edited by Adolfo Comerón, Evgueni I. Kassianov, Klaus Schäfer, Richard H. Picard, Karin Stein, John D. Gonglewski, Proc. of SPIE Vol. 9242, 92421I · © 2014 SPIE · CCC code: 0277-786X/14/$18 · doi: 10.1117/12.2070257

1. INTRODUCTION

Besides refraction, diffraction and aerosols the optical turbulence, represented by the structure function parameter of the refractive index C_n^2, is the main atmospheric influence on optical and electromagnetic wave propagation through the atmosphere. It is an important parameter in correcting images or estimating the performance of electro-optical systems operating with wavelengths in the visible of near infrared[1,2]. Applications include observing warning systems, laser communication links, laser beams and a lot of other military systems used for detection, recognition and identification. Because the most electro-optical systems are operated close to the ground, we will focus on the temporal and spatial distribution of optical turbulence in the atmospheric surface layer.

The atmospheric surface layer (ASL) is the lowest part of the turbulent atmospheric boundary layer with a vertical extension up to about 50 meter[3]. Due to the friction influence at the earth surface, this part of the atmosphere is especially affected by small-scale turbulence. The dominant size of turbulent eddies of the atmosphere increase with height because of the decreasing influence of the friction with height. Therefore C_n^2 shows a dependence on height in the atmosphere [4,5]. Many models exist trying to describe the decrease of C_n^2 with height. Some refer on a ground value of C_n^2 assuming an exponential decrease with height[4,6]. From the micrometeorological view, the atmospheric stability is used to describe the vertical profile of optical turbulence[5,7]. Besides the climatic and meteorological conditions also the kind of earth surface determines the strength of optical turbulence (water surface, vegetation, roughness)[8,9].

The focus of this work is set on the intercomparison of measurement techniques applied for determining optical turbulence. Hereby the main interest was set on the comparison between methods measuring the integrated turbulence along a path and single point measurements. Remote sensing systems like the SODAR-RASS (sound detection and ranging system Radio acoustic sounding system) are beyond the scope of this work because the application starts first at the top of the ASL.

Also there are remote sensing systems, which are often used for measuring the vertical distribution in the boundary layer or free troposphere or above. They are not so practical for the use in the atmospheric surface layer.

Published comparison experiments on different measurement systems in the ASL often deal with different methods measuring deep turbulence along a path[10]. Instrumental comparison of single-point measurements with integrated measurements are often directed towards the investigation of the sensible heat flux, regarding C_n^2 or C_T^2, the structure function of temperature, only as a side aspect[11].

For single point measurements the question of representativeness is critical, when the turbulence measurements should be applied for correcting electro-optical systems relying on their wave propagation through the atmosphere. For integrated or deep turbulence, a homogeneous distribution of turbulence along the path should prevail or the weighting function of the measurement technique should be known to attribute the measured turbulence to a certain height in case of a vertical or a slant path. In case of a heterogeneous environment, it is relevant which part will contribute most to the measured signal of optical turbulence.

So we will here focus on the comparison between single point measurements and integrated turbulence measurements. Therefore a close to ideal site was chosen in the Rietvlei Nature Reserve in South Africa south of Pretoria. The results of this field trial performed from the 18th to 30th June2013 are presented and analyzed with respect on the vertical behavior of the optical turbulence in the atmospheric surface layer. A description and overview on the whole field trial was given by Griffith[12].

2. DETERMINATION OF OPTICAL TURBULENCE IN THE ATMOSPHERIC SURFACE LAYER

Optical turbulence is an effect of mechanical and thermal forces in the atmosphere. Driven by solar radiation heating of the ground leads to buoyancy effects and therefore rising air parcels providing temperature variations in the atmosphere and therefore density fluctuations resulting in variations of the refractive index. These may also be caused by fluctuations in the water vapor density inferred by evapotranspiration at the ground from the surface or vegetation. But for wave propagation of wavelengths in the visible or IR humidity fluctuations play a minor role and can be ignored for land sites[13]. Over water bodies they might to be considered. Mechanical forces driven by wind shear will enhance or reduce optical turbulence dependent on the wind speed. This was investigated including a height dependency for a land station in the atmospheric surface layer by Sprung et al.[14].

Remote sensing systems like SODAR-RASS (sound detection and ranging – Radio acoustic sounding system) or LIDAR System may provide information about temperature variations (SODAR-RASS) or aerosol movement and the vertical distribution may be inferred from measuring the time of a sent out signal into the atmosphere. But of measuring the time difference between sent in incoming backscattered signal, the measurements normally start a few tens of meters above the surface and are therefore use for investigations of optical turbulence in the upper atmospheric boundary layer or free troposphere and will therefore not considered in this work. For a combination of supplementing instruments for investigation of the vertical distribution of optical turbulence in the lower atmospheric boundary layer (including SODAR-RASS measurement we refer to Sprung et al., 2011[14].

Here we follow the question how representative a measurement is or wherefrom the information originates, when integrated measurements are performed. Single point measurements have the difficulty to be only valid for a certain point in a chosen area. So that the single point has to be representative for this area. That is also the assumption in the whole Monin-Obukhov similarity theory (MOST)[15]. They may be also be affected by flow distortions (e.g. ultra sonic anemometers).

For investigating the optical turbulence and providing it for the design or application the accurate value of C_n^2 has to be known. For instruments like scintillometers, measuring the optical turbulence along a horizontal path between a transmitter and a receiver, the devices have a given weighting function. Figure 1 (left) shows the distribution of the weighting function for a large aperture scintillometer (BLS 900, Scintec, Rottenburg, Germany).

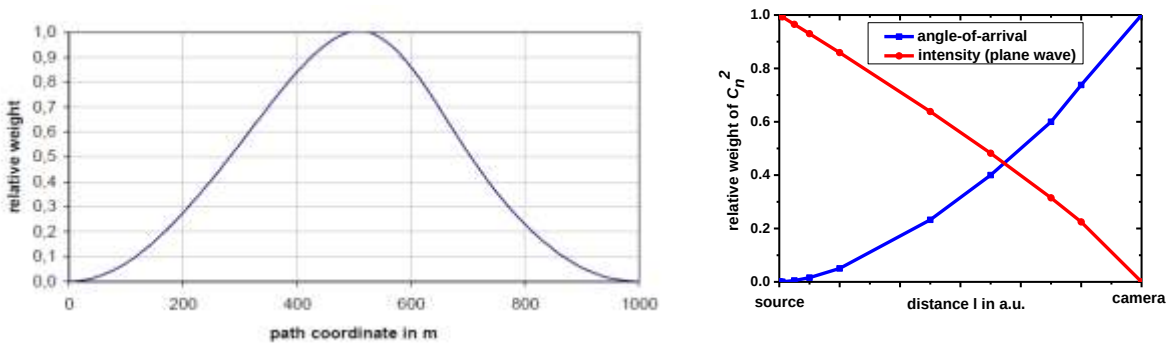

Figure 1. On the left hand side the instrumental weighting function of a large aperture scintillometer and on the right the weighting functions for telescope or camera measurements of a single spot light analyzing the beam wander (angle-of arrival method, blue) or using the scintillation (light intensity variations) technique (red).

For this instrument the signal of C_n^2 originates for the center of the measured path. So flow distortion may be caused by the transmitter or receiver will not effect the measurement of optical turbulence. For example it can be used for measurements above the sea using a bay for installation of the instrument.
In contrast the weighting function of telescopes or videography are shown. For example for monitoring a lamp with high speed (1000 fps), it depends on the analyzing technique. If the beam wander or angle-of arrival technique is used most of the signal of optical turbulence will come from area close to the camera (blue curve in figure 1, right). If the same sequence would be analyzed for variation in the scintillation of the monitored light, the signal of optical turbulence will come more from the side of the light. For analyzing such sequences for example along a slant path, with a significant difference between the height of the camera and the height of the light source, different strength of optical turbulence should be investigated.

The formula of the weighting function for the angle-of-arrival method is given[11] with

$$\left\langle \alpha^2 \right\rangle = 2.914 \cdot D^{-1/3} \cdot \int_0^L C_n^2(l) \cdot \left(\frac{l}{L} \right)^{5/3} dl \qquad (1).$$

With $<\alpha^2>$ as variance of the angle deviation α, wavelength λ, L the distance between source and sensor (path length) and l the position between light source and sensor (camera).
The weighting function for investigating the variance of the scintillation (intensity fluctuations) σ_I is also given by Laurent (1989)[11]

$$\sigma^2{}_I = 0.56 \cdot k^{7/6} \int_0^L C_n^2(l) \cdot (L-l)^{5/6} dl \qquad (2).$$

Using measurement along a slant path, these measurement techniques should give different results of optical turbulence along the same path.

3. EXPERIMENTAL SETUP

The experimental setup was given by Grifith[12] in detail. So here only the main aspects regarding the determination of optical turbulence are repeated. Measurements were performed above a Highveld grassland. The height of the dry grass was on average about 80 cm. The preliminary results[12] are reanalyzed.
The instrumentation for measurements of optical turbulence consisted of three ultra sonic anemometer (Gill HS-50, UK), one Surface-Layer Scintillometer (SLS 40, Scintec AG / Germany, hereafter only SLS), two Boundary-Layer Scintillometer (BLS 900, Scintec AG / Germany, hereafter only BLS) and a high speed camera (Redlake Motion Pro, DEL Imaging Systems LLC. / US), that monitors several lamps and LEDs mounted on a 30 m mast. Additional a weather station measuring the standard meteorological parameters including, visibility, radiation components, wind speed, wind direction and relative humidity are installed at 2 m height. Additional the soil surface temperature was measured.
The setup of the turbulence measurement is shown at figure 2.

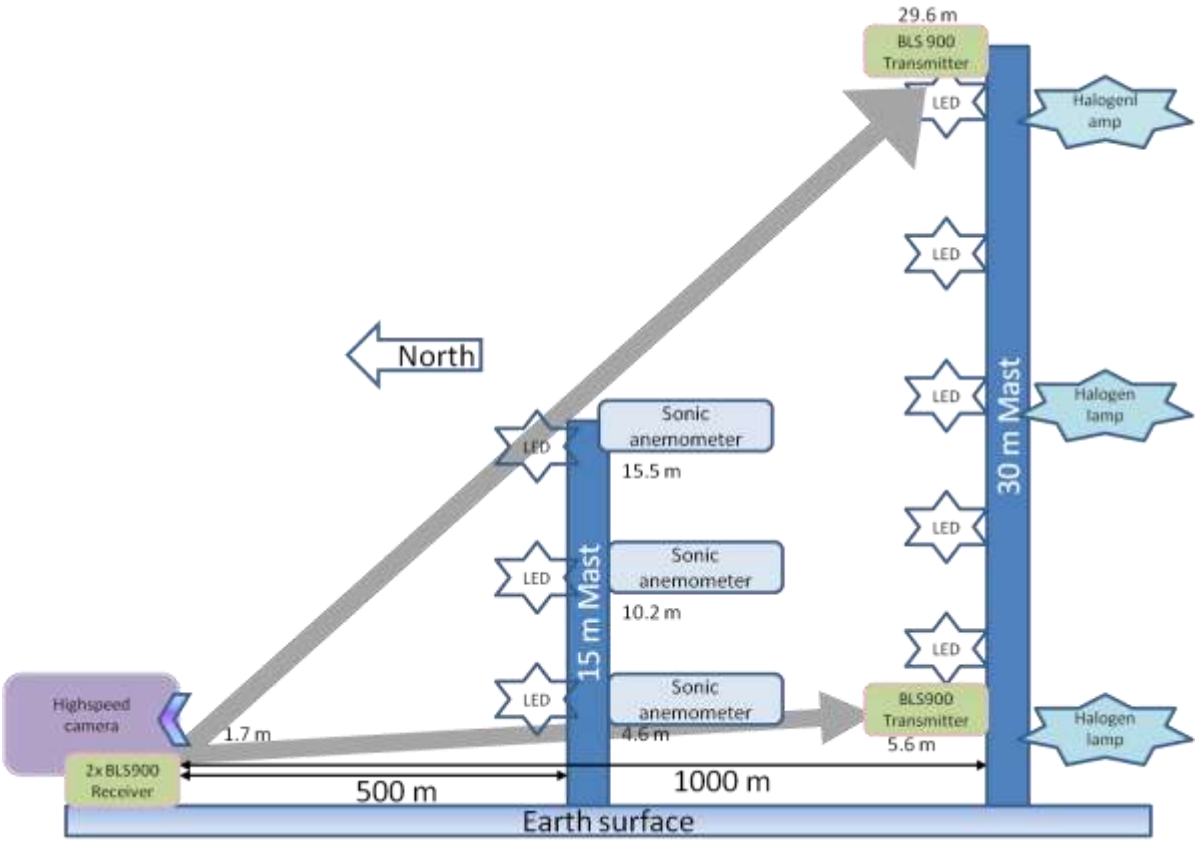

Figure 2. Setup measurement systems of the Rievlei campaign for measuring optical turbulence.

The distance of the integrated turbulence measurements was 1000 m. As ground reference the SLS was operated. It was used to determine the basic optical turbulence at 1.7 m above the surface horizontally over a distance of 100 m. It was operated along the path of 1000 m built up for the deep turbulence measurements. At the northern end receivers of the BLS systems and the camera were installed at a height of 1.7 m above ground. At the southern end a 30 m high lattice tower was set up. Here the transmitters of the BLS systems were installed at 5.6 m and 29.6 m height. Additionally five blue LEDs were mounted at 5.6 m, 11.6 m, 17.5 m 23.9 m and 28.9 m and three halogen lamps of 50 Watt at 5.6 m, 17.5 m and 28.9 m. In the center of the 1000 m path a movable mast of 15 m height was set up. Here the three sonic anemometers were mounted at 4.6 m, 10.2 m and 15.5 m aside with slow sensors for measurements of temperature and relative humidity.

The BLS is a system for measuring the integrated turbulence. Its weighting function is given in figure 2. The receiver was set at the northern end at 1.7 m height. The two detectors watch a dual disk 1000 m away on the 30 mast. One BLS looked at the source a height of 5.6 m with two disks of 924 LEDs with a wavelength of 880 nm. The other slant path for the second BLS was directed up to it transmitter at 28.9 m. So you get a geometric center for the lower path of 3.7 m, for the upper path of 15.7 m. The measurements were performed with a time resolution of 1 min. For comparison reasons towards the ultra-sonic anemometer. The data were averaged over 5 minutes.

The SLS system has the same principle of measurement like the BLS instead there is a laser beam of 670 nm as light source.

It was operated parallel along the mast line over a distance of 100 m, 1.7 m above ground. The time resolution was also 1 minute and the data were averaged over time periods of 5 minutes also for comparison reasons.
Three ultra sonic anemometers (HS-50, Gill, UK) were set up at the 15 m mast in the geometric center of the measurement path of the camera and BLS systems. Ultra sonic anemometers use the proportionality of the speed of sound on $\sqrt{T}$ (temperature T) to measure the sonic temperature T_s, that is close to the virtual temperature T_v [16]. Three pairs of senders and receivers send out a sound wave into both directions. From these 6 signals the three dimensional wind components may be determined. The three anemometers were mounted at the height of 4.6 m, 10.2 m and 15.5 m above the ground, directed to the west. The sampling frequency was 50 Hz. The three wind components u, v, w and the sonic Temperature T_s were monitored. From the time series 5 minute averages of C_T^2 were calculated performing a linear detrending, a coordinate rotation and Fast Fourier transformation on the data. For wavelengths in the visible and near infrared C_T^2 is proportional C_n^2 and C_n^2 can be determined using following formula [13]

$$C_n^2 = (79.2 \cdot 10^{-6} \frac{\overline{p}}{\overline{T}^2})^2 \cdot C_T^2 \qquad (3).$$

Was determined, using the simultaneously measured temperature T (in K) and pressure p (in hPa).
Also a camera (Motion Pro) was operated to make pictures of the 30 m mast with the 5 LEDs or 3 halogen lamps. Different frame rates and averaging times were chosen. The standard settings for comparison of the analyses of the videography, were an averaging time of 6 s and a frame rate of 2000 fps (frames per second). The sequences were analyzed using the angle-of-arrival (AOA) method. The optical turbulence C_n^2 is derived by

$$C_n^2 = \frac{\langle r \rangle^2 \cdot d^{1/3}}{1.09 \cdot L \cdot f^2} \qquad (4),$$

with r the radial deviation of the measured beam for small angles α, L the length of the measurement path between camera and source, f the focal length and d the aperture diameter.
These data were compared.

4. RESULTS AND DISCUSSION

For characterizing the measurements site and the prevailing meteorological conditions regarding the turbulent conditions the time series of the kinematic sensible heat flux w'T' and the friction velocity u_* are presented in figure 3. The friction velocity is the square root of the negative momentum flux. The sensible heat flux is a measure for the thermal force and the friction velocity for the mechanical force that drives the optical turbulence. Both were derived from the measurements with the ultra sonic anemometers. For the sensible heat flux the values of all three heights of the ultra sonic anemometer measurements are shown. Hardly any difference can be identified indicating a variation with height of less than 10 % as stated for the surface or constant flux layer[3]. At nighttime the fluxes are negative indicating a cooling from the ground and a sensible heat flux towards the ground. Maximum value of 0.3 K*m/s are reached, corresponding to a sensible heat flux of about 300 W/m² during the day. The friction velocity is noticeable during day and night. During the day up to 0.6 m/s are reached indicating strong mechanical turbulence. The conditions throughout the days of the measurement campaign show are steady and exhibit a very similar behavior for each day. These were good pre-conditions for an experiment for comparing measurement techniques. Both parameters are responsible for the development of optical turbulence as stated in chapter 2.

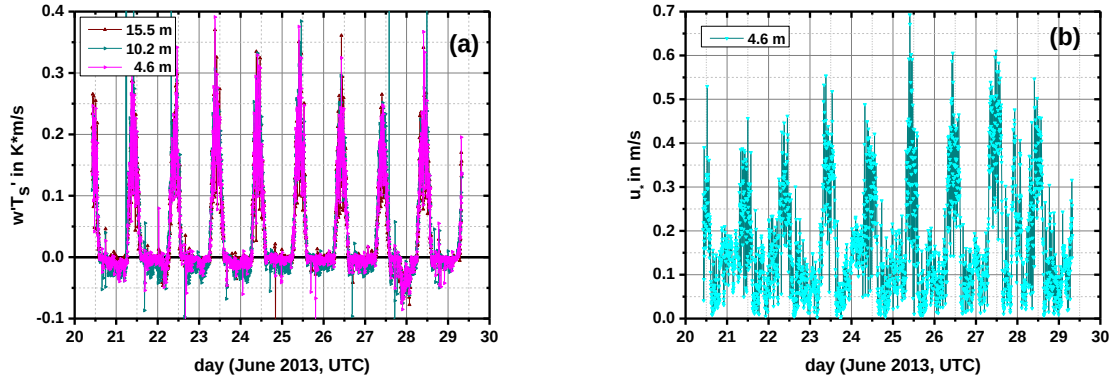

Figure 3. (a) Time series of the sensible heat flux for the three ultra sonic measurement heights 4.6 m (magenta),10.2 m (olive) and 15.5 m (purple) and (b) the friction velocity of 4. 6m during the Rietvlei campaign.

For the reference of optical turbulence close to the ground at a height of 1.7 m a SLS was operated with a path length of 100 m. The Time series from the 20th to the 30th June 2014 of these data, recorded with a time resolution of 1 min are presented in figure 4. The daily maxima of C_n^2 were about 10^{-12} $m^{-2/3}$. Minima at neutral atmospheric conditions decrease down to about $5*10^{-16}$ $m^{-2/3}$. Between sunrise at about 4:30 UTC and sunset 14:40 UTC a daily circle is pronounced. After the minimum at sunset until about 22:00 UTC C_n^2 increased again and reached values of C_n^2 of about $5*10^{-13}$ $m^{-2/3}$. After that time the optical turbulence mostly stayed below $2*10^{-13}$ $m^{-2/3}$. Close to the ground at this measurement height the turbulence seemed to be intermittent, expressed by the strong variations.

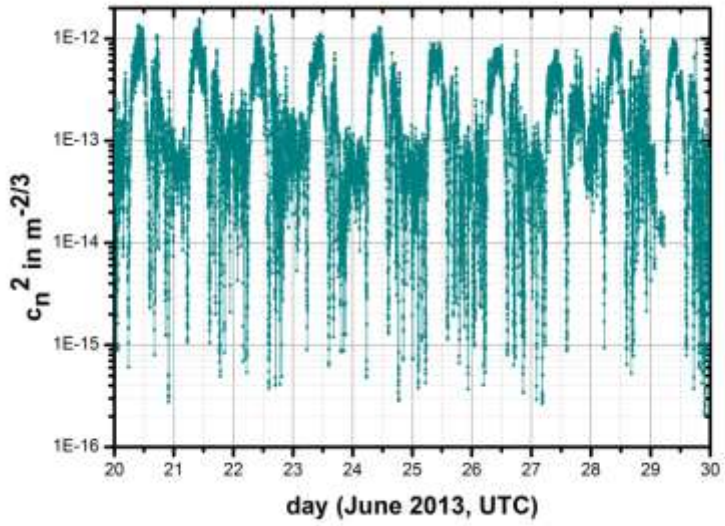

Figure 4. Time series of C_n^2 measures with the SLS at 1.7 m height above ground.

The strong temperature variations at winter time with daily maxima of 20 °C air temperature and night values around 0°C are analyzed[12]. They led to a strong heating and cooling of the ground.
This is more highlighted in figure 5 (a), showing the scattering of the optical turbulence as diurnal cycle of all data, now 5 min average for comparison the turbulence data calculated from the ultra sonic measurements. At figure 5 (a) additionally the data sets of the two slant path measurements with the Boundary Layer Scintillometers are presented. The one with a geometric height of 3.7 m in the center of the path is shown in olive, the second one with the center height of 15.7 m in brown. During unstable conditions during the day a strong decrease of C_n^2 with height is obvious. Also the delay in the development of turbulence after sunrise with height can be identified. In the beginning of the night optical turbulence developed from the ground after the equilibrium at sun set. That might be directed towards the development of a small inversion layer from the ground. A little bit mechanical turbulence (u_* in figure 3) exists responsible for the increase. From about 22:00 UTC an equilibrium in temperature is reached[12] and the turbulence kept constant at a lower level.

At figure 5 (b) the three diurnal cycles of the optical turbulence determined from the data of the ultra sonic anemometer measurements in 4.6 m (black), 10.2 m (red) and 15.5 m height (blue) are shown. There is a similar picture as in figure 5 (a).

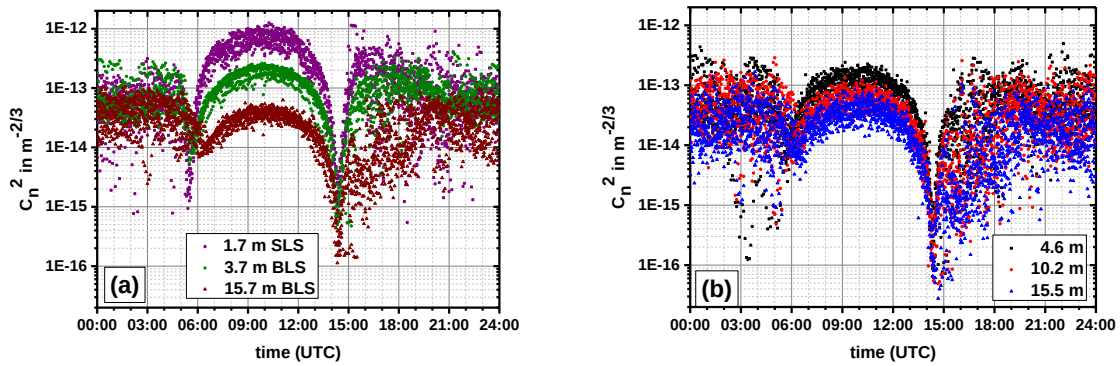

Figure 5: (a) diurnal cycle of scintillometer measurements of C_n^2 of the SLS at 1.7 m height (purple), the BLS of the lower slant path (olive) and the steeper slant path (brown) and (b) diurnal cycle of C_n^2 of the measurements with the ultra sonic anemometers at 4.6 m height (black), 10.2 m height (red) and 15.5 m height (blue).

The height dependence was analyzed with respect to the SLS measurements taken as ground value. For the convective conditions during the day for the ultra sonic anemometer at 10.2 m and 15.5 m height was found to depend on $h^{-4/3}$, like often stated in former publications. For the lowest sonic anemometer a decrease only with an exponent of -1.5 was calculated. For the stable nighttime conditions no factor of dependency was found. These dependencies on the decrease of turbulence were taken to estimate the height of the measurement of the BLS systems. The best fit was found for the calculated geometric heights of the center of the slant path, respectively 3.7 m for the lower BLS system and 15.7 m for the steeper slant path.
Taken this into account, at figure 6 now the different measurement techniques are compared for the lowest measurement heights. The time series from the 24th to 25th June is chosen. The general features can be identified as discussed for figure 6. At figure 7 the time optical turbulence at 1.7 m (SLS, blue), at 3.7 meter (BLS, magenta) and at 4.6 m (lowest ultra sonic anemometer, olive) are presented. For the BLS system the geometrical center of the slant path of 1000 m was assumed, because of the instrumental weighting function of the BLS system (figure 1). The receiver was set at 1.7 m and the transmitter at 28.9 m at the 30 m mast.

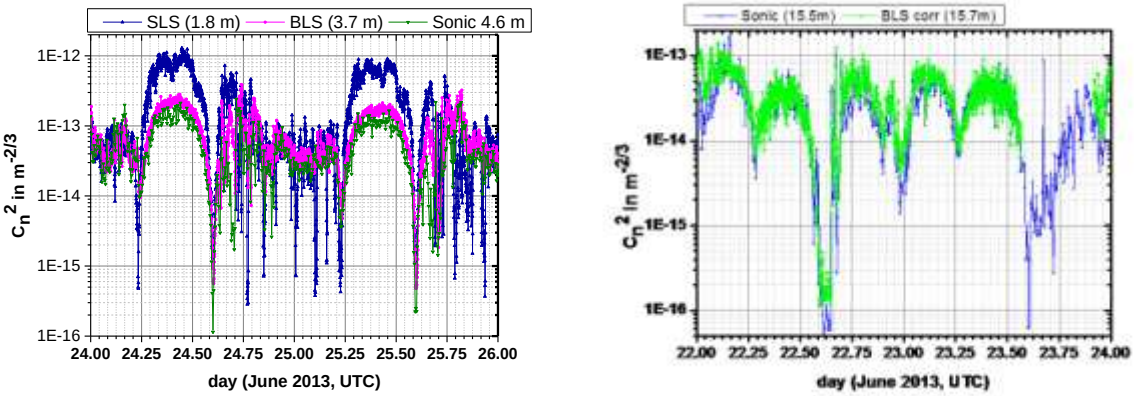

Figure 6. Time series of C_n^2 data from the 24th to 25th June 2014 of the Rietvlei campaign (blue, SLS data at 1.7 m height, magenta, BLS data at 3.7 m mean height, and olive, ultra sonic anemometer data at 4.6 m height). (b) Time series of C_n^2 data from the 22nd to 23rd June 2014 of the Rietvlei campaign (green BLS data at 15.7 m mean height, and blue ultra sonic anemometer data at 15.5 m height).

Because at night time the cooling rates between air and surface differ because of the different heat capacities, there seems to be an inversion layer staring from the ground, leading to optical turbulence increase after sunset. After 22:00 UTC an equilibrium in temperature seems to be reached and only the weak wind seems to produce mechanical turbulence. So no clear height dependency can be identified until sunrise. Close to the ground the turbulence seemed to be intermittent, creating the spikes below 10^{-15} $m^{-2/3}$ in the 1-min averages of the SLS 40 measurements. The single time series confirm the first statements of the results of the analysis of figure 6. This is in accordance with the statement on the weighting function of the BLS systems.

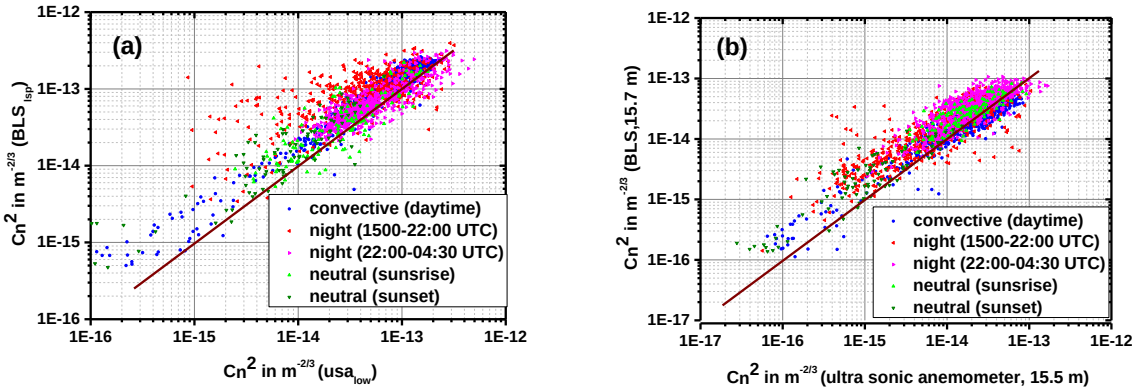

Figure 7: (a) C_n^2 value of the BLS measurement of the slant path with the center height of 3.7 m against the C_n^2 data of the sonic anemometer at 4.6 m height. The color coding indicates the stability regimes (unstable, convective in blue, stable conditions at night in red (1st half, and magenta 2nd half) and neutral conditions around sunrise in green and around sunset in olive). The straight line indicates the 1:1 line.(b) C_n^2 value of the BLS measurement of the slant path with the center height of 15. 7 m against the C_n^2 data of the sonic anemometer at 15.5 m height. The color coding indicates the stability regimes (unstable, convective in blue, stable conditions at night in red (1st half, and magenta 2nd half) and neutral conditions around sunrise in green and around sunset in olive). The straight line indicates the 1:1 line.

At figure 6 (b) the time series from the 22nd to 23rd June of the Rietvlei campaign of the ultra sonic anemometer data (blue) and the BLS for the steeper slant path are shown. The agreement between the two measurement systems is quite well, assuming that the measurement height is similar. At the evening of the 23rd June some BLS values were missing because of an instrumental power failure.

In figure 7 the data of the BLS systems are plotted against the ultrasonic anemometer data of optical turbulence to the closest heights to the geometric mean height of the slant path. The color coding indicates different stability levels of the atmosphere. In blue the convective unstable conditions during the day are indicated, in green and olive the neutral conditions during sunrise respectively sunset and in red or magenta the stable conditions during the night. In (a) the comparison was performed for the lower slant path measurement of the BLS system with a geometric mean level of 3.7 m and the ultra sonic anemometer data of the one at 4.6 m height. As expected and seen in figure 6 and 7 the BLS measurements show about 20 % higher values than the ultra sonic anemometer measurements because of the height difference. This was identified for the 5 classes of different stability regimes. The same was performed for the steeper BLS slant path system. There also the BLS data seems to show a little bit higher values than the sonic anemometer. The ratio between the measurement techniques keeps constant for the five stability classes. The BLS data seemed to show higher values than the sonic anemometer data of the same level.

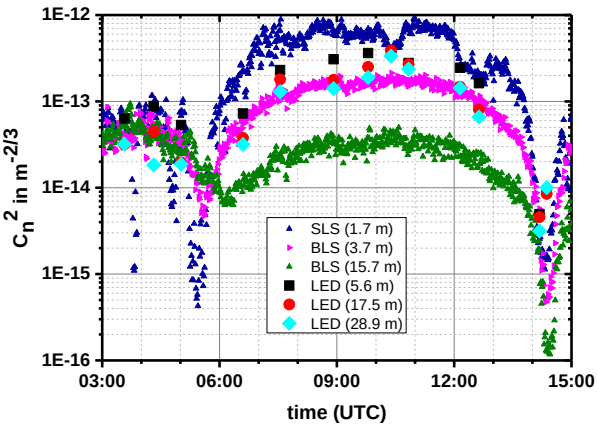

Figure 8: The scintillometer measurements of the 25th June 2014 from 3:00 UTC to 15:00 UTC (blue SLS at 1.7 m height, magenta BLS at mean height of 3.7 m and the BLS at 15.7 m mean height). The dots show the measurements of the high speed camera (at 1.7 m height) analyzed with the angle-of-arrival method (black square LED of 5.6 m, red point LED at 17.5 m, and cyan diamond at 28.9 m).

In figure 8 the comparison between high speed camera records and the scintillometer data was performed. The time series from 3:00 UTC to 15:00 UTC of the 25th June was analyzed. The high speed camera sequences were taken over time periods of 6 s with a frame rate of 1000 frames per second. 5 LEDs at the levels of 5.6 m, 11.2 m 17.5 m, 22.4, and 28.9 m were monitored simultaneously. In figure 9 the results of the heights of 5. 6 m (black), 17, 5m (red) and 28.9 m (cyan) are presented. For comparison the scintillometer data are also shown. The analyses were carried out using the angle-of-arrival method, i.d. the position of the center of the light maximum in the monitored picture was analyzed. The beam wander or dancing of the light was analyzed and the variances calculated using formula (4). The gradient of optical turbulence, the decrease of optical turbulence with height is also visible. But the strength of the signals was very close together. The strength of the calculated optical turbulence from the variance of the position of the maximum of the beam was for the

upper light identical with the signal of the BLS system of the lower slant path. Therefore the signal of the videography of the 4.6 m signal originates from about 3.7 m. The signal of the two lower lamps is a little bit higher, but not as high as the SLS signal. Using the height dependency of the optical turbulence to be assured, the signal indicates a height between 2 and 3 m above ground level. This would be in accordance with the weighting functions for telescope signals analyzing the position of the maximum of the monitored beams, the beam wander using the AOA-method. Comparing the same path of scintillometer systems and monitored light, the results differ a lot, indicating the difference introduced by the weighting function of the measurement systems.

5. CONCLUSIONS

Three measurement techniques have been compared in this article for measuring optical turbulence, the important atmospheric parameter affecting wave propagation of electro-optical systems. The point measurements of ultra sonic anemometer with the slant path measurements of BLS systems show a good agreement, attributing a reference height of the slant path measurement to its geometric height and mean level. Also vertical dependency of optical turbulence is clearly indicated with the different measurement techniques. The agreement of these two techniques worked well for all prevailing stability regimes in the atmospheric surface layer. Maximum values of about $2*10^{-12}$ $m^{-2/3}$ were during the reproducible steady conditions of the whole campaign between the 18th and 30th June and 1st July in the Nature Reserve of Rietvlei / South Africa.

The videography analyses show the strength of optical turbulence in accordance with the weighting function of the measurement technique. Besides the weak vertical resolution because of the signal strength close to the camera, also the height dependence is identified, analyzing the signals of 5 LEDs using the AOA-method. The results of three heights are presented and show the limited height resolution.

The analyses in the next step should be extended for analyzing the scintillation of the monitored LEDs. After the indicated weighting function for this method the signals should originate more from closer to the position of the light sources.

Analyzing the optical turbulence with different measurement techniques, besides the vertical distribution of optical turbulence in the atmospheric surface layer, also a lot of the horizontal distribution is possible to be identified. This measurement was a good start using the uniform terrain to overcome the difference between different measurement techniques. At all single point measurements agree very well even with integrated slant path measurements of optical turbulence.

Acknowledgement

We thank the German Federal Armed forces Technical Center (WTD91) for their financial support of this campaign in the frame of the ATLIMIS-project. Additional funding was provided by Armscor. The management of Rietvlei Nature Reserve is thankfully acknowledged for granting permission to use this area in the reserve. We also thank Master Towers for low-impact, timeous installation and removal of the 30m lattice mast. Fire warning services for the Rietvlei campaign were provided by the Advanced Fire Information System (AFIS8).

REFERENCES

[1] Tunick, A., "Toward increasing the accuracy and realism of future optical turbulence calculations", Meteorol. Atmos. Phys. Vol. 90, 159-164, (2005).

[2] Weiss-Wrana, K.R., "Turbulence statistics applied to calculate expected turbulence-induced scintillation effects on electro-optical systemsin different climate regions", Proc. of SPIE Vol. 5891, 5891D, (2005).

[3] Stull, R.B., [An introduction to boundary layer meteorology], Kluwer Academic Publishers, Dordrecht, (1988).

[4] Tatarskii V. I., [Wave propagation in a turbulent medium], McGraw-Hill Book C. inc., New York (1961).

[5] Wyngaard, J.C., Y. Izumi, and S.A. Collins Jr., "Behaviour of the refractive-index-structure parameter near ground", J. Opt. Soc. Am., Vol.61, p. 1646-1650, (1971).

[6] Hufnagel, R.E. and N.R. Stanley, J. Opt. Soc. Am., Vol. 54, No.52, (1964).

[7] Kunkel, K.E., D.L. Walters, and G.A. Ely, "Behaviour of the temperature structure parameter in a desert basin", J. Appl. Meteorol., Vol.20, p. 103-136, (1981).

[8] Weiss-Wrana, K.R. and L.S. Balfour, "Statistical analysis of measurements of atmospheric turbulence in different climates", Proc. of SPIE, (2002).

[9] Bendersky, S., N.S. Kopeika, and N. Blaustein, „Atmospheric optical turbulence over land in Middle East coastal environments: prediction modeling and measurements", Appl. Opt., Vol. 40, No.20, (2006).

[10] Laurent, J., G. Rousset, G. Fertin, J.F. Carlin, A. Kohnle, V. Thiermann, and M. Drumez, "Comparison between different techniques of turbulence measurements for horizontal path, Proc. of SPIE, Vol.1115, doi: 10.1117/1213723, (1989).

[11] Hartogensis, O.K., H.A.R. De Bruin; and B.J.H. van de Wiel, "Displaced-beam small aperture scintillometer test. PartII: CASES-99 stable boundary layer experiment", Boundary Layer Meteorology, Vol. 105, pp. 149-176, (2002).

[12] Griffith D., D.Sprung, E.Sucher, A. Ramkilowan, and L.Vhengani, "Comparison of slant-path scintillometry, sonic anemometry and high-speed videography for vertical profiling of turbulence in the atmospheric surface layer", Proc. SPIE 8890-14; doi: 10.1117/12.2032674, (2013).

[13] Hill, R.J., S.F. Clifford, and R.S. Lawrence, "Refractive-index and absorption fluctuations in the infrared caused by temperature, humidity, and pressure fluctuations", J. Opt. Soc. Am, 70, 1192-1205 (1980).

[14] Sprung, D., P. Grossmann, and E. Sucher, "Investigation of seasonal and diurnal cycles on the height dependence of optical turbulence in the lower atmospheric boundary layer", Proc. of SPIE 8517-39, (2012).

[15] Sprung, D., P. Grossmann, E. Sucher, K. Weiss-Wrana, and K. Stein „Stability and height dependant variations of the structure function parameters in the lower atmospheric boundary layer investigated from measurements of the long-term experiment VERTURM (vertical turbulence measurements)", Proc. of SPIE, 8178-8, (2011).

[16] Schotanus, P., F.T.M. Nieuwstadt, and H.A.R.de Bruin, "Temperature measurement with a sonic anemometer and its application to heat and moisture fluxes" , Boundary Layer Meteorology, 26, 81-93 (1983).